

# A comparison of perturbations in fluid and scalar field models of dark energy

H. K. Jassal<sup>1,\*</sup>

<sup>1</sup>*Harish-Chandra Research Institute, Chhatnag Road,  
Jhansi, Allahabad 211 019, India.*

We compare perturbations in a fluid model of dark energy with those in a scalar field. As compared to the  $\Lambda$ CDM model, large scale matter power spectrum is suppressed in fluid model as well as in a generic quintessence dark energy model. To check the efficacy of fluid description of dark energy in emulating a scalar field, we consider a potential which gives the same background evolution as a fluid with a constant equation of state. We show that for sub-Hubble scales, a fluid model effectively emulates a scalar field model. At larger scales, where dark energy perturbations may play a significant role, the fluid analogy breaks down and the evolution of matter density contrast depends on individual scalar field models.

PACS numbers: 98.80.-k, 95.36.+x, 98.65.-r

Cosmological observations have confirmed that the expansion of the universe is accelerating at present [1]. These observations include Supernova type Ia observations [2], observations of Cosmic Microwave Background [3, 4] and large scale structure [5]. The accelerated expansion of the universe can be explained by introducing a cosmological constant  $\Lambda$  in the Einstein's equation [6, 7, 8]. However, the cosmological constant model is plagued by the fine tuning problem [6]. This has motivated studies of dark energy models to explain the current accelerated expansion of the universe [9]. A typical feature of these models is that the dark energy density varies with time.

Varying dark energy is typically realized as an ideal fluid or as a scalar field. Purely from distance measurements, it is not possible to distinguish between different models with the same background evolution. Evolution of perturbations in these models is expected to break this degeneracy. In principle, Integrated Sachs Wolfe (ISW) effect can distinguish a cosmological constant from other models of dark energy, especially ones with a dynamical dark energy [10]. Dark energy perturbations have been extensively studied in the linear approximation [11, 12, 13, 14]. It was shown in [11] that dark energy perturbations affect the low  $l$  quadrupole in the CMB angular power spectrum through the ISW effect. For models with  $w > -1$  this effect leads to an enhancement in power while for phantom like models it leads to a suppression. Dark matter perturbations and dark energy perturbations are anti-correlated for large effective sound speeds. This anti-correlation is a frame dependent effect and vanishes if one considers dark energy rest frame instead of dark matter rest frame [12]. There are several other studies of perturbations in dark energy [15, 16], including some that deal with evolution of spherical perturbations: e.g. see Mota et al[17].

In this Brief Report we revisit dark energy perturbations in the context of a perfect fluid model and compare

the evolution with scalar field models. To describe dark energy perturbations, we choose the Newtonian gauge. In the absence of anisotropic stress, the perturbed metric can be written in the form

$$ds^2 = (1 + 2\Phi)dt^2 - a^2(t) [(1 - 2\Phi)\delta_{\alpha\beta}dx^\alpha dx^\beta] \quad (1)$$

where  $a(t)$  is the scale factor and  $\Phi$  is the gauge invariant potential defined in [18]. We have assumed the universe to be spatially flat. The Newtonian potential  $\Phi$  characterizes the metric perturbations.

The linearized perturbed Einstein equations for the above metric are given by

$$\begin{aligned} \frac{k^2}{a^2}\Phi + 3\frac{\dot{a}}{a}\left(\dot{\Phi} + \frac{\dot{a}}{a}\Phi\right) &= \quad (2) \\ &- 4\pi G [\rho_{NR}\delta_{NR} + \rho_{DE}\delta_{DE}] \\ \dot{\Phi} + \frac{\dot{a}}{a}\Phi &= -4\pi G [\rho_{NR}v_{NR} + \rho_{DE}v_{DE}] \\ 4\frac{\dot{a}}{a}\dot{\Phi} + 2\frac{\ddot{a}}{a}\Phi + \frac{\dot{a}^2}{a^2}\Phi + \ddot{\Phi} &= 4\pi G c_s^2 \rho_{DE} \delta_{DE} \end{aligned}$$

where dot denotes derivative with respect to the coordinate time  $t$ , with  $\rho_{NR}$  and  $\rho_{DE}$  representing energy density for nonrelativistic and dark energy components and  $P$  denotes pressure. The comoving velocity of a fluid or a field is denoted by  $v$ . Here  $\delta_{NR} \equiv \delta\rho_{NR}/\rho_{NR}$  is the density contrast for nonrelativistic matter and  $\delta_{DE}$  is the density contrast for dark energy. The symbol  $c_s^2 \equiv \delta P/\delta\rho$  denotes the speed of propagation of perturbations.

We first describe a fluid model of dark energy. For a fluid with a constant equation of state parameter  $w \equiv P/\rho$ , the continuity equation and Euler equation reduce to

$$\begin{aligned} \dot{\delta} &= (1 + w) \left[ -\nabla_\alpha v^\alpha + 3\dot{\Phi} - 3\frac{\dot{a}}{a}(c_s^2 - w)\delta \right] \quad (3) \\ \dot{v} &= \Phi + \frac{c_s^2}{1 + w}\delta + \frac{\dot{a}}{a}[3w - 1]v. \end{aligned}$$

It is useful to Fourier transform the above equations as in the linear regime the modes evolve independent of

\*<sup>a</sup>Email: hkj@hri.res.in

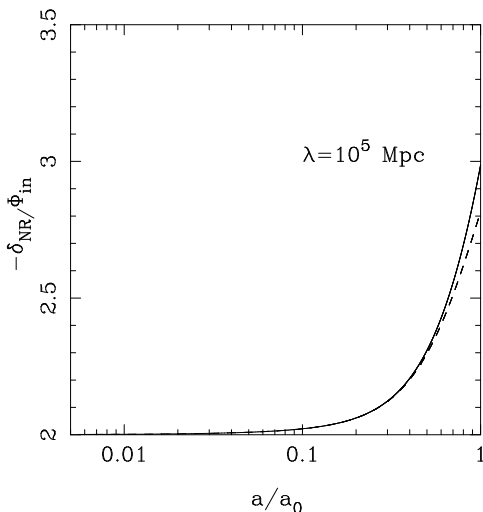


FIG. 1: The figure shows the evolution of density contrast for nonrelativistic matter (scaled by initial gravitational potential  $\Phi_{in}$ ) at  $\lambda = 10^5$  Mpc for the fluid model with  $w = -0.8$ . The solid line is evolution if we assume dark energy to be a smooth component of the universe. The dashed line is evolution of  $\delta_{NR}$  if dark energy clusters.

each other. Since we will discuss Fourier modes in the rest of the paper we do not use the subscript  $k$ .

For our discussion, we choose the following two equations

$$\begin{aligned} \Phi'' + 4\frac{\dot{a}}{a}\Phi' &= 4\pi G\rho_{DE}(c_s^2\delta_{DE} + 2w\Phi) \\ \delta_{DE}'' + (2 + 2c_s^2 - 6w)\frac{\dot{a}}{a}\delta_{DE}' + c_s^2\frac{\bar{k}^2}{a^2}\delta_{DE} \\ &- (c_s^2 - w)\left[\frac{3}{2}\frac{a'^2}{a^2} + \frac{3w}{2}\frac{\Omega_{DE}}{a^{3(1+w)}} + 9w\frac{a'^2}{a^2}\right]\delta_{DE} \\ &= (1+w)\left[-\frac{\bar{k}^2}{a^2}\Phi + 3(2-3w)\frac{a'}{a}\Phi' + 3\Phi''\right] \end{aligned} \quad (4)$$

We obtain the second equation by differentiating the first equation in (3) and eliminating  $v$ . The present day Hubble parameter is denoted by  $H_0$  and  $\Omega_{DE}$  is the density parameter for the dark energy component. The prime denotes derivative with respect to variable  $x = tH_0$  and  $\bar{k} = kc/H_0$ .

In the first equation in system (4), the  $\delta_{DE}$  term on the right hand side is the main departure from the concordance  $\Lambda$ CDM cosmology. If dark energy is a cosmological constant, then it does not cluster and the field  $\Phi$  decays whenever  $\Lambda$  dominates. For  $w \neq -1$ , the potential  $\Phi$  remains constant in the matter dominated era and starts to decay when dark energy contribution becomes significant. If  $c_s^2 = w$ , as soon as the dark energy component dominates, the effect of  $\delta_{DE}$  term is to increase the potential  $\Phi$ . This is a scale dependent effect and is more pronounced at small scales, i.e., for large  $k$  values. This increase is due to the fact that as dark energy starts to

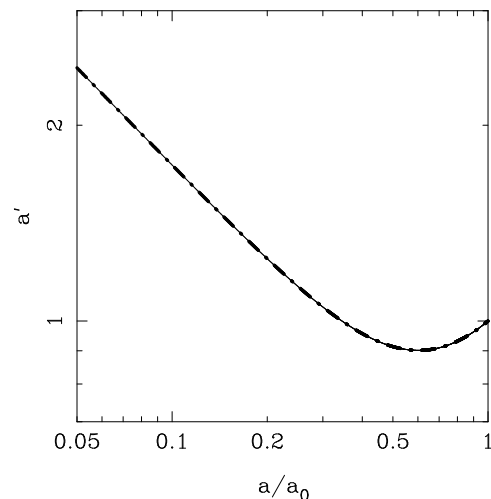


FIG. 2: The figure shows the evolution of  $a'$  as a function of  $a$ . The solid line is for a fluid model with  $w = -0.86$  and the dot dashed line is for the model with 'reconstructed' potential.

dominate, gradient in pressure enhances potential gradient and in turn dark energy clusters faster than matter [14]. For a positive sound speed, this instability is not there and the gravitational potential continues to decay in the dark energy dominated era.

In Fig. 1 we plot evolution of  $\delta_{NR}$  as a function of the scale factor  $a$  at length scale  $\lambda = 10^5$  Mpc. In this figure we fix the parameter  $c_s^2 = 1$ . At small scales, i.e., at length scales smaller than the Hubble radius, the evolution of the matter density contrast in perturbed dark energy scenario matches the evolution if dark energy is assumed to be homogeneous: due to a positive sound speed  $\delta_{DE}$  has an oscillatory behavior and these perturbations do not grow and hence matter perturbations behave as if dark energy is homogeneous. At large scales, as soon as dark energy starts to dominate, the difference starts to increase. Varying  $c_s^2$  does not make any difference as long as it is positive. In such a case there is no instability by way of a growing  $\Phi$ . The evolution of  $\Phi$  is the same for all  $\lambda <$  Hubble radius. The gravitational potential remains constant in the matter dominated era and starts to decay as dark energy dominates. At scales larger than the Hubble radius the decay of potential is slower. For models with  $w > -1$ , there is a correlation in dark energy density contrast and the matter density contrast. For 'phantom' models, these are anticorrelated, i.e. an overdensity in matter corresponds to an underdensity in dark energy. We will however consider only 'quintessence' type fields in this Report.

To differentiate between the role of background evolution and that of dark energy perturbations on matter perturbations, we choose a scalar field potential which emulates a constant dark energy equation of state. We call it the 'reconstructed' potential for further discussion. To emulate the background evolution corresponding to a

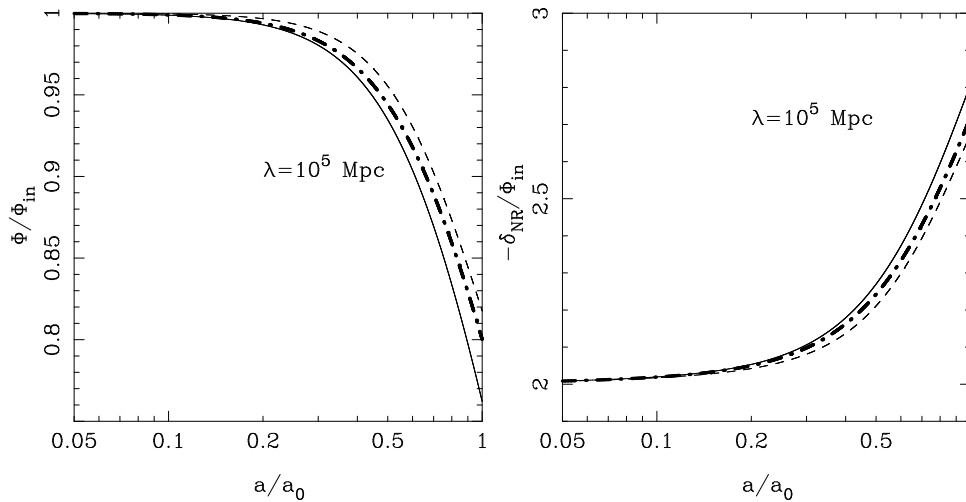


FIG. 3: The figure on the left shows the evolution of the gravitational potential  $\Phi$  as a function of  $a$  and the one on right shows matter density contrast for fluid model (solid line), for exponential potential (dashed line) and for the 'reconstructed' potential (thick dot dashed line) at  $\lambda = 10^5$  Mpc.

constant equation of state, the scalar field potential is given by [8, 20]

$$V(a) = \frac{3}{2}(1-w)H_0^2 M_P^2 \frac{\Omega_{DE}}{a^{3(1+w)}} \quad (5)$$

with evolution of scalar field  $\varphi$  given by

$$\frac{d\varphi}{da} = \frac{\sqrt{3(1+w)\Omega_{DE}M_P^2}}{a^{(5+3w)/2}\sqrt{\Omega_{NR}a^{-3} + \Omega_{DE}a^{-3(1+w)}}} \quad (6)$$

This potential gives the same background solution as that of a fluid with a constant  $w$  (as can be seen in Fig. 2). In the dark energy dominated era, it can be checked that the potential is an exponential one. We substitute the above in the perturbation equations for a scalar field

$$\delta\varphi'' + 3\frac{a'}{a}\delta\varphi' + \frac{\bar{k}^2\delta\varphi}{a^2} + 2\Phi\frac{dV(\varphi)}{d\varphi} - 4\Phi'\varphi' + \frac{d^2V(\varphi)}{d\varphi^2}\delta\varphi = 0 \quad (7)$$

and the linearized Einstein equation

$$\Phi'' + 4\frac{a'}{a}\Phi' + \left(2\frac{a''}{a} + \frac{a'^2}{a^2}\right)\Phi = 4\pi G \left[ \varphi'\delta\varphi' - \Phi\varphi'^2 \right. \\ \left. - \frac{dV(\varphi)}{d\varphi}\delta\varphi \right] \quad (8)$$

In the fluid model of dark energy, matter perturbations are suppressed as compared to the homogeneous dark energy model (this agrees with the result of [16] in the linear limit). This suppression is in contrast to the (quintessence) scalar field models where matter perturbations are enhanced by the presence of dark energy perturbations [19]. This difference is due to the fact the homogeneous limit is achieved differently for the two models. For a scalar field, even if one ignores spatial gradients

there still remains a contribution to  $\delta P$ . This contribution cancels with a corresponding contribution from the pressure term due to the background i.e., from the third term on the left hand side of Eq. 8. The cancellation of this term, for smooth dark energy, leads to a suppression in matter perturbations. This suppression is due to the assumption that dark energy is a smooth component. Therefore one must take care while taking this limit of quintessence models as the smooth limit is inconsistent. In other words, if dark energy is allowed to cluster the matter perturbations are enhanced in comparison. For fluid models  $\delta P$  vanishes and the residual pressure term due to the background evolution makes the evolution different from that in a scalar field. Therefore, assuming dark energy to be homogeneous leads to a large difference in matter density contrast. Perturbations increase the degeneracy between different models. As compared to the  $\Lambda$ CDM matter perturbations are suppressed for both fluid and for scalar field models.

We now compare the evolution of perturbations in the 'reconstructed' model with that in a fluid model. The fluid approximation works very well for sub-Hubble scales. The evolution of  $\delta_{NR}$  in this scalar field model is identical to the evolution in fluid model (with  $c_s^2 = 1$ ). This approximation breaks down at scales above the Hubble radius. The effects of the scalar field potential is dominant over that of the sound speed and  $\delta_{NR}$  closely follows that in the exponential potential.

In Fig. 3 we show the gravitational potential  $\Phi$  and  $\delta_{NR}$  as functions of  $a$  for fluid model, exponential potential  $V(\varphi) = V_0 \exp[-\sqrt{\alpha}\varphi/M_P]$  [19] ( $M_P$  being Planck mass), a fluid model with  $w = -0.86$  and the corresponding 'reconstructed' potential at  $\lambda = 10^5$  Mpc. For the exponential potential, if  $\alpha = 1$ , the dark energy equation of state  $w \approx -0.86$ . For small scales, say for

$\lambda = 50$  Mpc, the evolution in all three cases is very similar. At the present epoch, the percentage difference in the fluid model and the reconstructed potential model is less than  $10^{-5}\%$ . The difference between the fluid model and the exponential potential model is  $\approx 0.14\%$ . The reconstructed potential and fluid model start to differ on Hubble scale and larger. This difference remains less than  $1\%$  upto the scale  $\lambda = 10^4$ . For larger scales, i.e.,  $\lambda = 10^5$  Mpc, as soon as dark energy starts to dominate, the behavior of reconstructed potential model becomes closer to that of an exponential potential. The percentage difference in the fluid model and the reconstructed potential model is  $\approx 3.6\%$  and the difference between the reconstructed potential and the exponential potential model is  $\approx 0.8\%$ . The dominant term in time evolution of  $\delta_{NR}$  in both the cases is  $\dot{a}^2\Phi/a^2$ . The other terms suppress this evolution and these terms are model dependent with the scalar field potential and its derivatives having a more pronounced effect in this opposition than in the fluid model. At large scales therefore, in the dark energy dominated epoch, the properties of the scalar field potential come into play.

The results of this work are summarized as follows. Dark energy perturbations in fluid models suppress matter perturbations as compared to the corresponding smooth dark energy model. Matter perturbations are suppressed as compared to the  $\Lambda$ CDM model. As long as the sound speed is positive the evolution of matter perturbations is indistinguishable from a smooth dark energy model. This is true for scales smaller than the Hubble radius. Dark energy perturbations in a fluid model emulate that of a scalar field model very well below the Hubble scale but start to differ at larger scales. Therefore the fluid model is not a good approximation at these scales. This also implies that the growth of perturbations at large scales depends on the details of the model even though the background evolution is the same. A separate analysis is therefore required for every model.

The author is grateful to J. S. Bagla, T. Padmanabhan, T. R. Seshadri, K. Subramanian and S. Unnikrishnan for useful discussion. The author thanks Department of Science and Technology, India for financial assistance through project number SR/WOS-A/PS-11/2006.

- 
- [1] J. P. Ostriker and P. J. Steinhardt, *Nature (London)* **377**, 600 (1995); S. D. M. White, J. F. Navarro, A. E. Evrard and C. S. Frenk, *Nature (London)* **366**, 429 (1993); J. S. Bagla, T. Padmanabhan, and J. V. Narlikar, *Comments on Astrophysics* **18**, 275 (1996); G. Efstathiou, W. J. Sutherland, and S. J. Maddox, *Nature (London)* **348**, 705 (1990); H. K. Jassal, J. S. Bagla and T. Padmanabhan, *astro-ph/0601389*; U. Alam, V. Sahni and A. A. Starobinsky, *JCAP* **0702**, 011 (2007).
- [2] P. Astier *et al.*, *Astron. Astrophys.* **447**, 31 (2006) [*astro-ph/0510447*].
- [3] A. Melchiorri *et al.*, *Astrophys. J.* **536**, L63 (2000).
- [4] E. Komatsu *et al.*, E. Komatsu, *et al.*, *ApJS*, **180**, 330 (2009)
- [5] W. J. Percival *et al.*, *ApJ* **657**, 645 (2007)
- [6] S. Weinberg, *Rev. Mod. Phys.* **61**, 1 (1989).
- [7] T. Padmanabhan, *Phys. Rep.* **380**, 235 (2003); P. J. Peebles and B. Ratra, *Rev. Mod. Phys.* **75**, 559 (2003); J. Ellis, *Phil. Trans. Roy. Soc. Lond. A* **361**, 2607 (2003); T. Padmanabhan, *Curr. Sci.* **88**, 1057 (2005).
- [8] V. Sahni and A. Starobinsky, *Int. J. Mod. Phys. D* **9**, 373 (2000).
- [9] E. J. Copeland, M. Sami, S. Tsujikawa, *Int. J. Mod. Phys. D* **15**, 1753 (2006) [*hep-th/0603057*]; V. Sahni, *astro-ph/0403324*; T. Padmanabhan, *arXiv:0705.2533* [*gr-qc*]; T. Padmanabhan, *AIP Conf. Proc.* **861**, 179 (2006).
- [10] J. B. Dent, S. Dutta and T. J. Weiler, *Phys. Rev. D* **79**, 023502 (2009).
- [11] J. Weller and A. M. Lewis, *Mon. Not. Roy. Astron. Soc.* **346**, 987 (2003).
- [12] R. Bean and O. Dore, *Phys. Rev. D* **69**, 083503 (2004).
- [13] N. Bartolo, P. S. Corasaniti, A. R. Liddle and M. Malquarti, *Phys. Rev. D* **70**, 043532 (2004); W. Hu, *Phys. Rev. D* **71**, 047301 (2005); C. Gordon, *Nucl. Phys. Proc. Suppl.* **148**, 51 (2005); C. Gordon and D. Wands, *Phys. Rev. D* **71**, 123505 (2005); L. R. Abramo and F. Finelli, *Phys. Rev. D* **64**, 083513 (2001); J. Grande, A. Pelinson and J. Sola, *Phys. Rev. D* **79**, 043006 (2009); O. Sergijenko, Yu. Kulinich, B. Novosyadlyj and V. Pelykh, *arXiv:0809.3349* [*astro-ph*]; B. Novosyadlyj and O. Sergijenko, *arXiv:0808.2098* [*astro-ph*]; P. P. Avelino, L. M. G. Beca and C. J. A. Martins, *Phys. Rev. D* **77**, 101302 (2008); R. Mainini, *JCAP* **0807**, 003 (2008); D. F. Mota, J. R. Kristiansen, T. Koivisto and N. E. Groeneboom, *Mon. Not. Roy. Astron. Soc.* **382**, 793 (2007).
- [14] C. Gordon and W. Hu, *Phys. Rev. D* **70**, 083003 (2004).
- [15] J. C. Fabris, S. V. B. Goncalves and P. E. de Souza, *Gen. Rel. Grav.* **34**, 53 (2002); W. Zimdahl and J. C. Fabris, *Class. Quant. Grav.* **22**, 4311 (2005); S. Silva e Costa, M. Ujevic and A. Ferreira dos Santos, *arXiv:gr-qc/0703140*; V. Gorini, A. Y. Kamenshchik, U. Moschella, O. F. Piattella and A. A. Starobinsky, *arXiv:0711.4242* [*astro-ph*].
- [16] S. Dutta and I. Maor, *Phys. Rev. D* **75**, 063507 (2007); I. Maor and O. Lahav, *JCAP* **0507** (2005) 003; P. Wang, *Astrophys. J.* **640**, 18 (2006); D. F. Mota and C. van de Bruck, *Astron. Astrophys.* **421**, 71 (2004); N. J. Nunes and D. F. Mota, *Mon. Not. Roy. Astron. Soc.* **368**, 751 (2006); C. Horellou and J. Berge, *Mon. Not. Roy. Astron. Soc.* **360**, 1393 (2005); L. R. Abramo, R. C. Batista, L. Liberato and R. Rosenfeld, *JCAP* **0711**, 012 (2007); R. Mainini, *JCAP* **0904**, 017 (2009).
- [17] D. F. Mota, D. J. Shaw and J. Silk, *arXiv:0709.2227* [*astro-ph*], D. F. Mota, *JCAP* **09**, 006 (2008).
- [18] J. Bardeen, *Phys. Rev. D* **22**, 1882 (1980) H. Kodama and M. Sasaki, *Prog. Theor. Phys. Suppl.*, **78**, 1 (1984). V. F. Mukhanov, H. A. Feldman and R. H. Brandenberger, *Phys. Rep.* **215**, 203 (1992).

- [19] S. Unnikrishnan, H. K. Jassal and T. R. Seshadri, Phys. Rev. D **78**, 123504 (2008).
- [20] C. Quercellini, M. Bruni and A. Balbi, arXiv:0706.3667; S. Unnikrishnan, Phys. Rev. D **78**, 063007 (2008).